Acta Pharmacologica Sinica

www.nature.com/aps

ARTICLE

Disfunction of dorsal raphe nucleus-hippocampus serotonergic-HTR3 transmission results in anxiety phenotype of Neuroplastin 65-deficient mice

Jie Cheng[1,2], Ling Chen[1,2], Ya-ni Zheng[1,2], Juan Liu[3], Lei Zhang[1,2], Xiao-ming Zhang[1,2], Liang Huang[1,2] and Qiong-lan Yuan[1,2]✉

Anxiety disorders are the most common psychiatric condition, but the etiology of anxiety disorders remains largely unclear. Our previous studies have shown that neuroplastin 65 deficiency (NP65$^{-/-}$) mice exhibit abnormal social and mental behaviors and decreased expression of tryptophan hydroxylase 2 (TPH2) protein. However, whether a causal relationship between TPH2 reduction and anxiety disorders exists needs to be determined. In present study, we found that replenishment of TPH2 in dorsal raphe nucleus (DRN) enhanced 5-HT level in the hippocampus and alleviated anxiety-like behaviors. In addition, injection of AAV-NP65 in DRN significantly increased TPH2 expression in DRN and hippocampus, and reduced anxiety-like behaviors. Acute administration of exogenous 5-HT or HTR3 agonist SR57227A in hippocampus mitigated anxiety-like behaviors in NP65$^{-/-}$ mice. Moreover, replenishment of TPH2 in DRN partly repaired the impairment of long-term potentiation (LTP) maintenance in hippocampus of NP65$^{-/-}$ mice. Finally, we found that loss of NP65 lowered transcription factors Lmx1b expression in postnatal stage and replenishment of NP65 in DRN reversed the decrease in Lmx1b expression of NP65$^{-/-}$ mice. Together, our findings reveal that NP65 deficiency induces anxiety phenotype by downregulating DRN-hippocampus serotonergic-HTR3 transmission. These studies provide a novel and insightful view about NP65 function, suggesting an attractive potential target for treatment of anxiety disorders.

Keywords: neuroplastin 65; dorsal raphe nucleus; tryptophan hydroxylase 2; Lmx1b; serotonergic transmission; anxiety disorders

Acta Pharmacologica Sinica (2024) 0:1–13; https://doi.org/10.1038/s41401-024-01252-5

INTRODUCTION

Anxiety disorders are the most common psychiatric condition, afflicting three in ten people worldwide. Individuals with anxiety disorders are excessively fearful, anxious, or avoidant of perceived threats in the environment in their daily lives, and the lifetime prevalence rate exceeds 20% [1]. However, the etiology of anxiety disorders remains largely unclear. Interestingly, our previous studies have shown that neuroplastin 65 deficiency (NP65$^{-/-}$) mice exhibit anxiety-like behaviors [2, 3], and the underlying mechanism needs to be explored.

Neuroplastin (Nptn), as a member of the cell adhesion molecules, is a major glycoprotein component of the synaptic membrane [4–6]. NP65 and NP55, two isoforms of Nptn, are only distinguished by the presence of the extracellular Ig1 module in NP65 but its absence in NP55 [4, 6, 7]. NP65 is mainly and abundantly expressed in brain and involved in synaptic plasticity, whereas NP55 is widely expressed in various tissues in rodents [7, 8]. Recently, accumulating evidence has shown that Nptn is implicated in neuropsychiatric disorders [2, 3, 9]. Bhattacharya and colleagues reported that constitutive Nptn$^{-/-}$ mice (both NP65 and NP55 deleted) showed anxiolytic-like behaviors in two paradigms: open-field test (OFT) and light-dark transition (LDT) test, and depressive-like behaviors in the tail suspension test. In contrast, the adult inducible Nptn$^{-/-}$ mice displayed normal behaviors in OFT and LDT test [9], indicating that the deletion of Nptn in adulthood did not affect anxiety-like behaviors in mice. Interestingly, we found that constitutive NP65$^{-/-}$ mice clearly displayed anxiogenic-like behaviors in several paradigms: OFT, LDT, hole-board test and marble burying test, which was reproduced by different individuals in our lab [2, 3]. In addition, NP65$^{-/-}$ mice showed less depressive-like behaviors in tail suspension test, but comparable depressive-like behaviors in forced swim test and sucrose preference test, compared to control littermates [2]. Furthermore, Nptn$^{-/-}$ (constitutive and inducible) mice and NP65$^{-/-}$ mice displayed no difference in motor ability [2, 3, 9]. Given that NP65 is brain-specific and anxiety phenotype of Np65$^{-/-}$ mice is identified in different paradigms, it is necessary to uncover the potential mechanisms for how the loss of NP65 leads to anxiety-like behaviors in mice.

The serotonergic or 5-hydroxytryptamine (5-HTergic) system is implicated in a wide range of behaviors, including emotional behaviors such as anxiety- and depression-like behaviors [10–14], and the response to rewards [15, 16]. In brain, the 5-HTergic neurons are specifically located in the raphe nuclei of brainstem [17, 18] and project to nearly every area of the forebrain including the cerebral cortex and hippocampus, constituting serotonergic

[1]Department of Neurology, Shanghai Tongji Hospital, Tongji University School of Medicine, Shanghai 200065, China; [2]Department of Human Anatomy, Histology and Embryology, Tongji University School of Medicine, Shanghai 200092, China and [3]Chinese Institute for Brain Research, Beijing 102206, China
Correspondence: Qiong-Lan Yuan (yqiongl@tongji.edu.cn)

Received: 10 November 2023 Accepted: 26 February 2024
Published online: 25 March 2024

synaptic transmission to affect neuropsychiatric behaviors [19–21]. 5-HTergic neurons are distributed in nine distinct raphe nuclei in the brainstem [18], of which the dorsal raphe nucleus (DRN) contains about 35% of total 26,000 serotonin-producing neurons in the mouse brain and constitutes approximately 70% serotonergic input to the forebrain [17, 18, 22]. Tryptophan hydroxylase 2 (TPH2) is a rate limiting enzyme for 5-HT synthesis in brain, and specifically expressed in raphe nuclei in brainstem [23]. It is well known that altered 5-HT level in forebrain is involved in anxiety- and depression-related behaviors [2, 24–28]. In addition, diversity of 5-HT receptors (HTR) also determines the distinct emotional behaviors in different condition [29, 30]. Among 14 types of 5-HT receptors identified so far [30], HTR3 is the only ligand-gated ionotropic receptor [31]. A wealth of evidence has shown that HTR is required for normal emotional response. For example, HTR1 subunit A mutant mice show elevated anxiety and antidepressant-like behavior [32]; HTR3 subunit A (HTR3A) mutant mice produce an anxiolytic phenotype [33]. HTR3A is required for functional HTR3 and is expressed in a subpopulation of gamma aminobutyric acid interneurons of hippocampus and cortex in rodents [20, 31]. Coincidentally, we found significant decreases in 5-HT level in hippocampus, the expression of TPH2 protein in raphe nuclei, and the expression of forebrain HTR3A in NP65$^{-/-}$ mice [2, 34]. Therefore, these previous results suggest that altered serotoninergic system in brain could be related with anxiety-disorders in NP65$^{-/-}$ mice.

In this study, we aimed to determine a direct causal relationship between the disturbed serotoninergic system and anxiety-like behaviors in NP65$^{-/-}$ mice. To this end, after injected with AAV-TPH2-GFP or AAV-NP65-GFP in DRN, or given with exogenous 5-HT in hippocampus or HTR3 agonist, Np65$^{-/-}$ mice were followed to perform a serials of anxiety-like behavior tests. Finally, our study provides direct evidence that the reduced serotonergic-HTR3 transmission from DRN to hippocampus contributes to the anxiety phenotype of NP65$^{-/-}$ mice.

MATERIALS AND METHODS

Animals

Homozygous NP65$^{-/-}$ mice were generated as previously described [3]. Wild-type C57BL/6 mice (WT mice) from the same background strain were used as controls in all experiments. All mice were housed under a 12 h light–dark cycle with the temperature at 23–25 °C and food/water ad libitum. All procedures were in accordance with an animal protocol approved by Tongji University Animal Care Committee.

Preparation of viruses overexpressing NP65 or TPH2

The vector for overexpressing mouse NP65 is AAV-hSyn-NP65-EGFP-3FLAG-SV40 Poly A (AAV-NP65), and the control is AAV-MCS-EGFP-3FLAG-SV40 Poly A(AAV-CON). These viruses were constructed and packaged by Genechem Technology (Shanghai, China) as follows: AAV9-NP65 (8.67×10^{12} V.G/ mL) (AAV-NP65), AAV9-CON (8.71×10^{12} V.G/mL) (AAV-CON). The vector for overexpressing mouse Tph2 is AAV9-hSyn-TPH2-P2A-GFP(AAV-TPH2), and the control is AAV-hSyn-GFP (AAV-GFP). These viruses were generated by WZ Biosciences Inc (Jinan, Shandong, China) as follows: AAV9-TPH2 (8.89×10^{13} V.G/mL) (AAV-TPH2), AAV9-CON (7.71×10^{13} V.G/mL) (AAV-CON).

Intracerebral injection of AAV-NP65, AAV-TPH2, 5-HT and HTR3 agonist SR57227A

WT and NP65$^{-/-}$ mice (8- to 9-week-old) were anaesthetized by intraperitoneal injection of pentobarbital sodium (80 mg/kg, Sigma-Aldrich, St. Louis, MO, USA) for administration of AAV-NP65, AAV-TPH2 and 5-HT, or by 2% isoflurane for administration of SR57227A, and then placed in a stereotaxic frame (Alcott Biotect CO., LTD, Shanghai, China). Burr holes (0.5 mm in diameter) were drilled targeting for DRN according to the coordinates (AP: −4.7 mm; ML: 0 mm, DV: −3.0 mm) or for bilateral stratum radiatum of the CA1 area of hippocampus (AP: −2.2 mm, ML: ±1.6 mm, DV, −1.9 mm). 1 μL of viral solution containing AAV-NP65 (2.17×10^9 V.G) or AAV-TPH2 (1.11×10^9 V.G) was injected into the DRN at a speed of 0.2 μL /min using a 10 μL Hamilton syringe. For controls, l μL of viral solution containing AAV-CON was delivered, respectively.

For 5-HT or HTR3 agonist SR57227A injection in hippocampus, 5-HT (20 μg/1 μL, H9523; Sigma, CA, USA) or SR57227A (15 pg/1 μL, HY-102064, MedChemExpress, New Jersey, USA) was injected bilateral hippocampus at a speed of 0.2 μL /min into the mouse brain. As a control, 1 μL of saline was injected. The dose of 5-HT and SR57227A was determined based on the previous reports [35–37] and our preliminary experiments. At the end of injection, the needle was left in place for additional 5 min before it was slowly withdrawn.

Four weeks after viral injection, mice treated with AAV-TPH2 or AAV-NP65 in DRN were subjected to a serials of anxiety-like behavioral tests as indicated in Figs. 2a or 3a, and then brain samples were collected. After 60 min for 5-HT infusion or 20 min for SR57227A injection in hippocampus as described previously [35, 37, 38], the mice were tested in a serials of anxiety-like behavioral paradigms as shown in Figs. 2e and 4d.

Anxiety-like behavioral tests

In this study, these mice treated with AAV-NP65, AAV-TPH2, 5-HT or SR57227A as above mentioned were subjected to anxiety-like behaviors. These typical paradigms for assessing anxiety-like behaviors including OFT, elevated plus maze (EPM) test and LDT test [39–41] were successively performed by a blinded investigator.

For OFT, a cubic arena (50 cm × 50 cm × 50 cm), made of light-gray plastics, was used. On day 1, each mouse ($n = 7$–8 mice/group) was placed in a cubic arena for habituation for 5 min. On day 2, each mouse was randomly placed in one of the four corners of the arena and allowed to freely explore the whole arena for 5 min. The mouse traveling paths were recorded by video camera. The velocity, the time spent in the center zone (25 cm × 25 cm in the middle of the cubic arena) and number of entries into the center zone were measured and analyzed with EthoVision software (Noldus, Shanghai, China). After each test, the arena was thoroughly cleaned with 70% ethanol to remove any odor.

The EPM apparatus was comprised of two open arms (65 cm × 5 cm) and two closed arms (65 cm × 5 cm × 20 cm) elevated 50 cm above the ground. The intersection of the arms was defined as center area (10 cm ×10 cm). Mice were placed in the center area facing one of the two open arms and allowed to explore for 5 min. The traveled paths of mice were recorded by video camera. The time spent in the open arms and number of entries into the open arms were counted and analyzed with EthoVision software (Noldus, Shanghai, China). After each test, the arena was thoroughly cleaned with 70% ethanol.

The LDT apparatus was composed of a plastic cage (60 cm × 40 cm × 50 cm) divided into small (one third) dark and large (two thirds) light compartments connected by a door. Mice were placed in the illuminated compartments and allowed to freely move between the dark and light compartments for 5 min. All trials were recorded digitally for subsequent offline analysis by a blinded investigator. Entering the light compartment was considered only if mice had two front paws and half of the body into the compartment. The trajectory of mouse movement was recorded by video camera. After each test, these compartments were cleaned with 70% ethanol.

Enzyme-linked immunosorbent assay (ELISA)

The hippocampus, frontal cortex and DRN were dissected out from WT + AAV-CON mice, NP65$^{-/-}$ + AAV-CON mice and NP65$^{-/-}$ +

AAV-TPH2 mice. After mice were euthanized with pentobarbital sodium, the whole brain tissues were rapidly taken out and placed on the ice. Frontal cortex was firstly taken out. After overlying temporal cortex was unveiled, the hippocampus was exposed and collected for use. For DRN tissue, midbrain was separated and cut coronally from the occipital pole of cerebral hemisphere and 1 mm posterior to here. DRN tissue, about 1 mm × 2 mm in size below the central aqueduct of the midbrain, was cut and collected for use. Brain tissues were weighed and lysed in ELISA tissue extract buffer with an amount of 300 μL per 5 mg tissue using Serotonin ELISA Kit (Ab133053, Abcam, Cambridge, UK). Tissue lysis was then centrifuged at 10,000 × *g* at 4 °C for 15 min to obtain the supernatant. Then, the supernatant was added to the 96-well plate, followed by incubating with serotonin antibody for 2 h. Finally, the stop solution was added and the absorbance of each well was immediately measured at a wavelength of 405 nm. The 5-HT concentration of each sample was calculated by drawing a standard curve based on the concentration of serotonin standards and their absorbance.

Western blotting

After mice were euthanized with pentobarbital sodium (200 mg/kg), brain tissues were rapidly removed and frozen until further analysis. Bilateral hippocampus and DRN tissues were isolated, lysed and centrifuged at 10,000 × *g* at 4 °C for 10 min and the supernatant was collected. After determining the protein concentration, protein samples (20 μg) per lane were electrophoretically separated in 10% sodium dodecyl sulfate-polyacrylamide gels and then transferred to polyvinylidene fluoride membranes. These membranes were blocked with 5% BSA in TBS containing 0.05% Tween-20 for 1 h at room temperature (RT), and were incubated overnight at 4 °C with primary antibodies including goat anti-NP65 (1:500, AF5360, R&D Systems, Minnesota, USA), rabbit anti-TPH2 (1:1000, Ab184505, Abcam, Cambridge, UK), rabbit anti-Lmx1b (1:200; GTX129831, GeneTex, CA, USA) and mouse anti-HTR3A (sc390168, Santa Cruz Biotechnology, TX, USA) and rabbit anti-GAPDH (AG019, Beyotime, Shanghai, China). Membranes were then washed and incubated with anti-rabbit IgG-HRP, anti-goat IgG-HRP or anti-mouse IgG-HRP (1:1000, Beyotime) for 2 h at RT. Immunoreactive bands were visualized and images were analyzed quantitatively using ImageJ software (NIH, Bethesda, USA). Protein levels were normalized to those of GAPDH from two or three independent experiments.

Quantitative real-time PCR (qRT-PCR)

Total RNA was extracted from the DRN in WT and NP65$^{-/-}$ mice using TRIzol reagent (Thermo Fisher Scientific, Waltham, MA, USA). RNA concentration was measured using a spectrophotometer (ND-1000, NanoDrop Technologies, Rockland, DE, USA). cDNA synthesis was performed with 2 μg RNA and 2 μL Evo M-MLVRT Master Mix (AG11706, Accurate Biotechnology, Hunan, China). The cDNA synthesis condition was as follows: 37 °C for 15 min; 85 °C for 5 s. Quantitative PCR was performed with 2 μL cDNA on the 7300 Real Time PCR system (Applied Biosystems, Foster City, CA, USA) using an TB Green Premix Ex Taq^{TM} II (RR820B, Takara, Japan). The PCR condition was as follows: initial denaturation, 95 °C for 5 min; 40 cycles of denaturation (95 °C for 30 s), annealing (56 °C for 30 s), and elongation (72 °C for 60 s). mRNA levels were analyzed by the ΔΔCt method. Primers used in the study were listed as follows: TPH2: forward primer (5′-GTGACCCTGAATCC GCCTG-3′), reverse primer (5′-GGTGCCGTACATGAGGACT-3′); Lmx1b: forward primer (5′-TTCCTGATGCGAGTCAACGAG-3′), reverse primer (5′-TCCGATCCCGGAAGT AGCAG-3′); Pet1: forward primer (5′-ACGCCTACCGCTTTGACTTC-3′), reverse primer (5′-AAGC TGCCATCAAGTTGAGTT-3′); GAPDH: forward primer (5′-TG ACCTCAACTACATGGTCTACA-3′), reverse primer (5′-CTTCCCATTC TCGGCCT TG-3′).

Immunofluorescence Staining

After deeply anesthetized with pentobarbital sodium, mice were transcardially perfused with 0.9% saline followed by 4% paraformaldehyde. Brains were then removed and fixed in the same fixative for 24 h at 4 °C, and then placed sequentially in 20% and 30% sucrose (in 0.1 M PBS, pH 7.4) at 4 °C for dehydration until brain sank to the bottom of the bottle. Consecutive coronal sections of brain tissues containing dorsal hippocampus and midbrain (25 μm thick) were prepared using a cryostat microtome (model 1950, Leica, Wetzlar, Germany). For TPH2, Lmx1b and HTR3A immunostaining, brain sections were permeabilized with PBST (0.1 M PBS with 0.3% Triton-X 100) for 30 min and then blocked with PBST containing 5% goat serum for 1 h at RT. Then, sections were incubated overnight at 4 °C with the primary antibodies: rabbit anti-TPH2 (1:200; Ab184505, Abcam), rabbit anti-Lmx1b (1:200; GTX129831, GeneTex, CA, USA) and rabbit anti-HTR3A (1:200; Ab13897, Abcam). Then sections were washed three times in PBST and incubated with Cy3-conjugated goat anti-rabbit secondary IgG (1:500; A0516, Beyotime) for 2 h at RT. Especially, for HTR3A immunostaining, sections were incubated with biotinylated horse anti-rabbit secondary IgG (1:500; BA1100, Vector Laboratories, Newark, CA, USA) for 3 h at RT, followed by incubation with Cy3-conjugated streptavidin (1:1000, 016-160-084, Jackson ImmunoResearch Laboratories). Finally, after three washes with PBST, sections were mounted with antifade mounting medium containing 4′,6-diamidino-2-phenylindole (DAPI, 1:1000; P0131, Beyotime, Shanghai, China) and imaged by a confocal fluorescence microscope (Olympus FV1000, Tokyo, Japan). For quantification of immunopositive areas or immunopositive cells, seven for (DRN) and five to seven (for dorsal hippocampus) brain sections covering the DRN or hippocampus were selected from an individual mouse ($n = 3$ mice /group). Quantitation was performed manually in a double-blinded manner.

For 5-HT/TPH2 and 5-HT/NP65 double immunostaining after viral microinjection, the brain slices were firstly exposed to bright light at room temperature for two days to quench the fluorescence of green fluorescent protein and then followed to the procedures similar to TPH2/NP65 immunostaining for brain slices of wild type mice. Brain sections were treated with sodium citrate buffer (pH = 6.0) at 95 °C for 5 min in a water bath. After blocked with PBST containing 5% goat serum for 1 h at RT, sections were simultaneously incubated overnight at 4 °C with both primary antibodies: goat anti-NP65 (1:200; AF5360, R&D Systems, Minnesota, USA) and rabbit anti-TPH2 (1:200; Ab184505, Abcam); goat anti-5-HT (1:200; 20081, ImmunoStar) and rabbit anti-TPH2 (1:200; Ab184505, Abcam); rabbit anti-5-HT (1:200; S5545, Sigma) and goat anti-NP65 (1:200; AF5360, R&D Systems, Minnesota, USA). After washing with PBST, sections were incubated with biotinylated horse anti-goat secondary IgG (1:500; BA9500, Vector Laboratories, Newark, CA, USA) for 3 h at RT, followed by incubation with Cy3-conjugated streptavidin (1:1000, 016-160-084, Jackson ImmunoResearch Laboratories) and Alexa Fluor 488-conjugated goat anti-rabbit secondary IgG (1:500; A0423, Beyotime). Finally, after washing thoroughly, sections were mounted with antifade mounting medium containing DAPI and imaged by a confocal microscope (Olympus FV1000, Tokyo, Japan).

Electrophysiological recordings for LTP of hippocampal slice

Four weeks after injecting AAV-TPH2 or AAV-CON as above described, mice were anesthetized with isoflurane and decapitated. Brains were rapidly removed and placed in ice-cold oxygenated artificial cerebral spinal fluid (aCSF) (95% O_2 and 5% CO_2): NaCl, 124 mM; $NaHCO_3$, 25 mM; KCl, 4.4 mM; KH_2PO_4, 1 mM; $CaCl_2$, 2 mM; $MgSO_4$, 2 mM; Glucose, 10 mM at 28–30 °C for at least 1 h before recording. Coronal 300 μm-thick hippocampal slices were cut in ice-cold aCSF using a vibrating microtome (Leica, VT1000S; Germany). Slices were transferred to a recovery chamber

with oxygenated (95% O_2 and 5% CO_2) aCSF for at least 1.5 h at RT until recordings were performed.

For LTP, slices were transferred to a recording chamber and submerged in aCSF for 5 min before recording. Slices were then laid down in a chamber with 8 × 8 microelectrode array (Parker Technology, Beijing, China) in the bottom planar (each 50 μm × 50 μm in size, with an interpolar distance of 150 μm) and kept submerged in aCSF. Signals were obtained using a Multi Clamp 700B amplifier (Axon 700B, MD, Sunnyvale, CA, USA) under visual control with differential interference contrast illumination on an upright microscope (BX51WI; Olympus).

Field excitatory postsynaptic potentials (fEPSP) in CA1 neurons were recorded by stimulating CA3 neurons. LTP was induced by applying three trains of high-frequency stimulation (HFS: 100 Hz, 1–3 duration). The LTP magnitude was quantified as the percentage changes in the fEPSP (10%–90%) taken during the 60-min interval after LTP induction.

Statistical analysis

All statistical analyses were performed using SPSS statistics software v18 (IBM, Armonk, NY, USA). Data are expressed as means ± standard error of mean (SEM). Unpaired Student's *t* tests were used to evaluate the difference between two groups. Multiple comparisons were performed using one-way analysis of variance followed by the Fisher's least significant difference test if the data are in normal distribution. Otherwise, the Dunnett's T3 test was used to determine the significance among multiple comparisons. Differences were considered statistically significant when the *P*-value was <0.05.

RESULTS

Administration of AAV-TPH2 in DRN or exogenous 5-HT in hippocampus alleviates anxiety-like behaviors in NP65$^{-/-}$ mice

To reveal the relationship between TPH2 reduction and anxiety-like behaviors in NP65$^{-/-}$ mice, we administrated AAV-TPH2 into DRN (Fig. 1a) and synthesized neurotransmitter 5-HT into CA1 subarea of hippocampus in NP65$^{-/-}$ mice to observe whether the anxiety-like behaviors would be mitigated. Firstly, Western blotting analysis showed that AAV-TPH2 administration significantly increased the TPH2 expressions in the DRN of NP65$^{-/-}$ mice four weeks after injection ($F_{2,6} = 5.218$, $P = 0.041$, Fig. 1b, c). Consistently, 5-HT/TPH2 double immunostaining also showed that the number of the TPH2- and 5-HT- immunopositive cells was significantly elevated in NP65$^{-/-}$ mice injected with AAV-TPH2 comparing that in NP65$^{-/-}$ mice injected with AAV-CON (NP65$^{-/-}$ control, TPH2-immunopositive cells: $F_{2,6} = 65.314$, $P < 0.001$; 5-HT-immunopositive cells: $F_{2,6} = 42.774$, $P = 0.001$; Fig. 1d–f). Moreover, the merger of 5-HT/TPH2 immunostaining showed that TPH2 immunoreactivity was overlapped with 5-HT immunoreactivity in DRN of the WT and NP65$^{-/-}$ controls (Fig. 1d–g). Whereas a few of TPH2 immunoreactive neurons of DRN did not overlap with 5-HT immunoreactivity in NP65$^{-/-}$ mice treated with AAV-TPH2, indicating that few of TPH2-positive neurons may not produce 5-HT. In addition, quantitative analysis showed that the ratio of TPH2/5-HT immunoreactive neurons to TPH2 immunoreactive neurons was about 90% in the DRN of the NP65$^{-/-}$ mice treated with AAV-TPH2 (Fig. 1d–g). These results indicate majority of TPH2 positive neurons produce 5-HT in NP65$^{-/-}$ mice treated with AAV-TPH2. Notably, the TPH2-immunoreactive bands and TPH2-immunospositive cells in the DRN of NP65$^{-/-}$ mice injected with AAV-TPH2 nearly reached their levels in WT mice injected with AAV-CON (WT control, bands: $F_{2,6} = 5.218$, $P = 0.722$; cells: $F_{2,6} = 6.895$, $P = 0.913$, Fig. 1b–e). Moreover, TPH2-immunopositive axonal terminals in hippocampus were significantly increased in NP65$^{-/-}$ mice injected with AAV-TPH2 relative to that in the NP65$^{-/-}$ control ($F_{2,6} = 9.103$, $P = 0.021$) and were comparable to that in WT control ($F_{2,6} = 5.523$, $P = 0.706$, Fig. 1h, i). These results indicate that AAV-TPH2 administration in DRN significantly enhances the TPH2 expressions in DRN and hippocampus of NP65$^{-/-}$ mice, suggesting that AAV-TPH2 injection may enhance the serotonergic projections of the DRN to the hippocampus. Furthermore, the level of 5-HT in hippocampus, DRN and frontal cortex were assessed using ELISA analyses. As shown in Fig. 1j, k, 5-HT concentrations were comparable in the frontal cortex between NP65$^{-/-}$ and WT control ($F_{2,9} = 0.784$, $P = 0.335$), but significantly decreased in the hippocampus in NP65$^{-/-}$ mice ($F_{2,9} = 10.362$, $P = 0.011$), which is consistent with our previous report [2]. As expected, 5-HT concentrations in the hippocampus and DRN were significantly increased in NP65$^{-/-}$ mice injected with AAV-TPH2 compared with those in the NP65$^{-/-}$ control (hippocampus: $F_{2,9} = 10.362$, $P = 0.011$; DRN: $F_{2,9} = 11.739$, $P = 0.002$), and nearly reached their levels in the WT control (hippocampus: $F_{2,9} = 10.362$, $P = 0.053$; DRN: $F_{2,9} = 11.739$, $P = 0.843$, Fig. 1k, l). Meanwhile the 5-HT level was unaltered in frontal cortex ($F_{2,9} = 0.784$, $P = 0.284$, Fig. 1j) in NP65$^{-/-}$ mice between the injection with AAV-TPH2 or control virus. We also observed that NP65$^{-/-}$ control and WT control exhibited similar 5-HT levels in frontal cortex ($F_{2,9} = 0.784$, $P = 0.335$, Fig. 1j), consistent with our previous report [2]. Taken together, these results demonstrate that the administration of AAV-TPH2 in the DRN in NP65$^{-/-}$ mice reverses the decrease in TPH2 expression in DRN and results in an increase in 5-HT level in the DRN and hippocampus of NP65$^{-/-}$ mice.

Because the AAV-TPH2 replenished the expression of TPH2 and the concentration of 5-HT of the DRN and hippocampus in NP65$^{-/-}$ mice, we thus explored whether anxiety-like behaviors would be changed by administration of AAV-TPH2 four weeks later (Fig. 2a). In the OFT, AAV-TPH2 partly reversed the decrease in the time spent in the central zone ($F_{2,21} = 16.839$, $P = 0.006$), and the number of entering the central zone ($F_{2,21} = 49.708$, $P = 0.039$) in NP65$^{-/-}$ mice, whereas the speed of movement was unaffected among these groups (Fig. 2b). Similarly, in the EPM test, the AAV-TPH2 treatment partly prevented the decrease in the time spent in the open arms ($F_{2,21} = 15.323$, $P = 0.008$) and the number of entering the open arms ($F_{2,21} = 18.568$, $P = 0.013$) in NP65$^{-/-}$ mice (Fig. 2c). In the LDT test, AAV-TPH2 significantly increased the number of entries into the light box ($F_{2,21} = 8.136$, $P = 0.011$) and the duration in the light box ($F_{2,21} = 29.362$, $P = 0.016$) in NP65$^{-/-}$ mice relative to NP65$^{-/-}$ control (Fig. 2D). In addition, NP65$^{-/-}$ control mice showed anxiety phenotype compared with WT controls in OFT, and EPM and LDT (Fig. 2b–d), as we previously reported [2, 3].

To further determine if reduced 5-HT level in hippocampus would result in anxiety phenotype in NP65$^{-/-}$ mice, we performed these behavioral tests in NP65$^{-/-}$ mice 60 min after they were given exogenously synthesized neurotransmitter 5-HT (20 μg) into the hippocampus (Fig. 2e, f). In the OFT, exogenous 5-HT in hippocampus significantly increased the time spent in the central area ($F_{2,21} = 40.82$, $P = 0.02$) and the number of entries into the central zone ($F_{2,21} = 26.068$, $P = 0.02$) in NP65$^{-/-}$ mice, although they were still lower than those in the WT control (treated with saline; time: $F_{2,21} = 40.82$, $P < 0.001$; entries: $F_{2,21} = 26.068$, $P < 0.001$). Meanwhile, the movement ability was unaltered among different groups (Fig. 2g). In the EPM test, exogenous 5-HT in some extent reversed the decrease in time spent in the open arms ($F_{2,21} = 31.144$, $P = 0.021$) and the number of entries into the open arms ($F_{2,21} = 35.727$, $P = 0.002$) in NP65$^{-/-}$ mice (Fig. 2h). Lastly, the LDT test showed that the administration of 5-HT in hippocampus prevented the decrease in the number of entries into the light box ($F_{2,21} = 26.528$, $P = 0.005$) and the time spent in the light box ($F_{2,21} = 29.362$, $P = 0.016$) in NP65$^{-/-}$ mice (Fig. 2i).

Taken together, these results indicate that the anxiety-like behaviors in NP65$^{-/-}$ mice are partially due to the reduced serotonergic transmission of the DRN to the hippocampus. Replenishing the TPH2 expression in DRN or injecting exogenous 5-HT in the hippocampus can partly alleviate anxiety-like behaviors

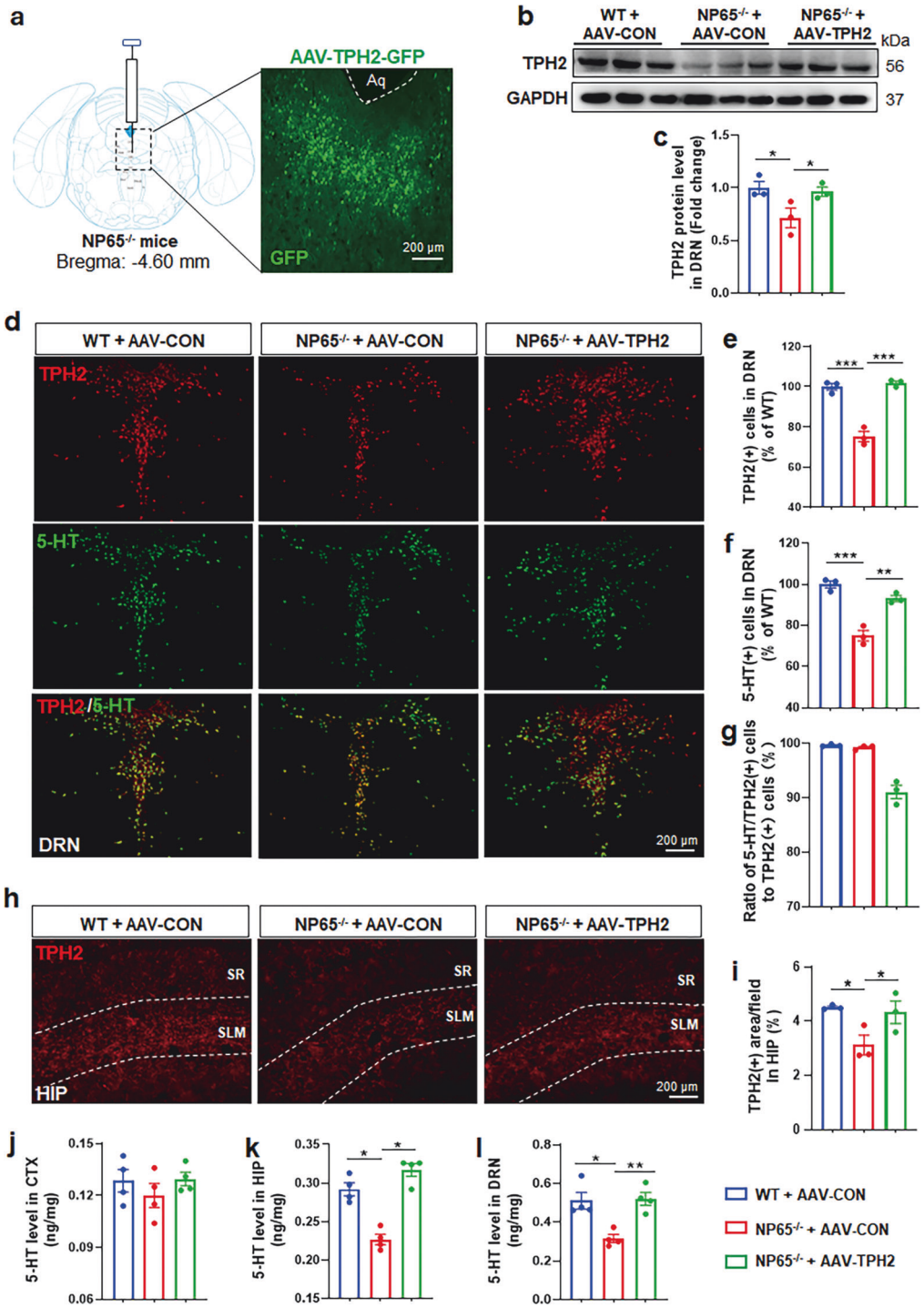

Fig. 1 Injection of AAV-TPH2 in DRN increases TPH2 and 5-HT level in NP65$^{-/-}$ mice. a Schematic of virus injection in DRN, as indicated by GFP (green) under fluorescence microscopy 4 weeks after virus injection. 100× magnification, Scale bar = 200 μm. Representative immunoreactive bands (**b**) and quantitative analysis (**c**) showing TPH2 levels in the DRN of NP65$^{-/-}$ and WT mice (n = three mice/group). Representative micrographs of the TPH2/5-HT double immunostaining in DRN (**d**) and quantifications (**e**–**g**) show expression the levels of TPH2 and 5-HT from WT and NP65$^{-/-}$ mice (**d**–**f**), and the merged images (**d**) of TPH2/5-HT double immunostaining and quantification (**g**) (n = 3 mice/group). 100× magnification, Scale bar = 200 μm. Representative micrographs of the TPH2 positive axonal terminals of stratum lacunosum molecular (SLM) and stratum radiatus (SR) in the hippocampus (HIP, **h**) and Quantification (**i**) in WT and NP65$^{-/-}$ mice. ELISA analyses show 5-HT concentrations in the frontal cortex (CTX, **j**), hippocampus (**k**) and DRN (**l**) in WT and NP65$^{-/-}$ mice (n = 4 mice/group). Data are presented as mean ± SEM. *P < 0.05; **P < 0.01, ***P < 0.001.

in NP65$^{-/-}$ mice. Meanwhile, our results also suggest that other potential mechanisms involved in the anxiety-like behaviors may exist in NP65$^{-/-}$ mice besides the decrease in serotonergic synaptic transmission of the DRN to the hippocampus.

Administration of AAV-NP65 in DRN increases TPH2 expression and alleviates anxiety-like behaviors in NP65$^{-/-}$ mice

To figure out whether the reduction of TPH2 expression in DRN is due to NP65 deficiency, we administered AAV-NP65 in DRN of

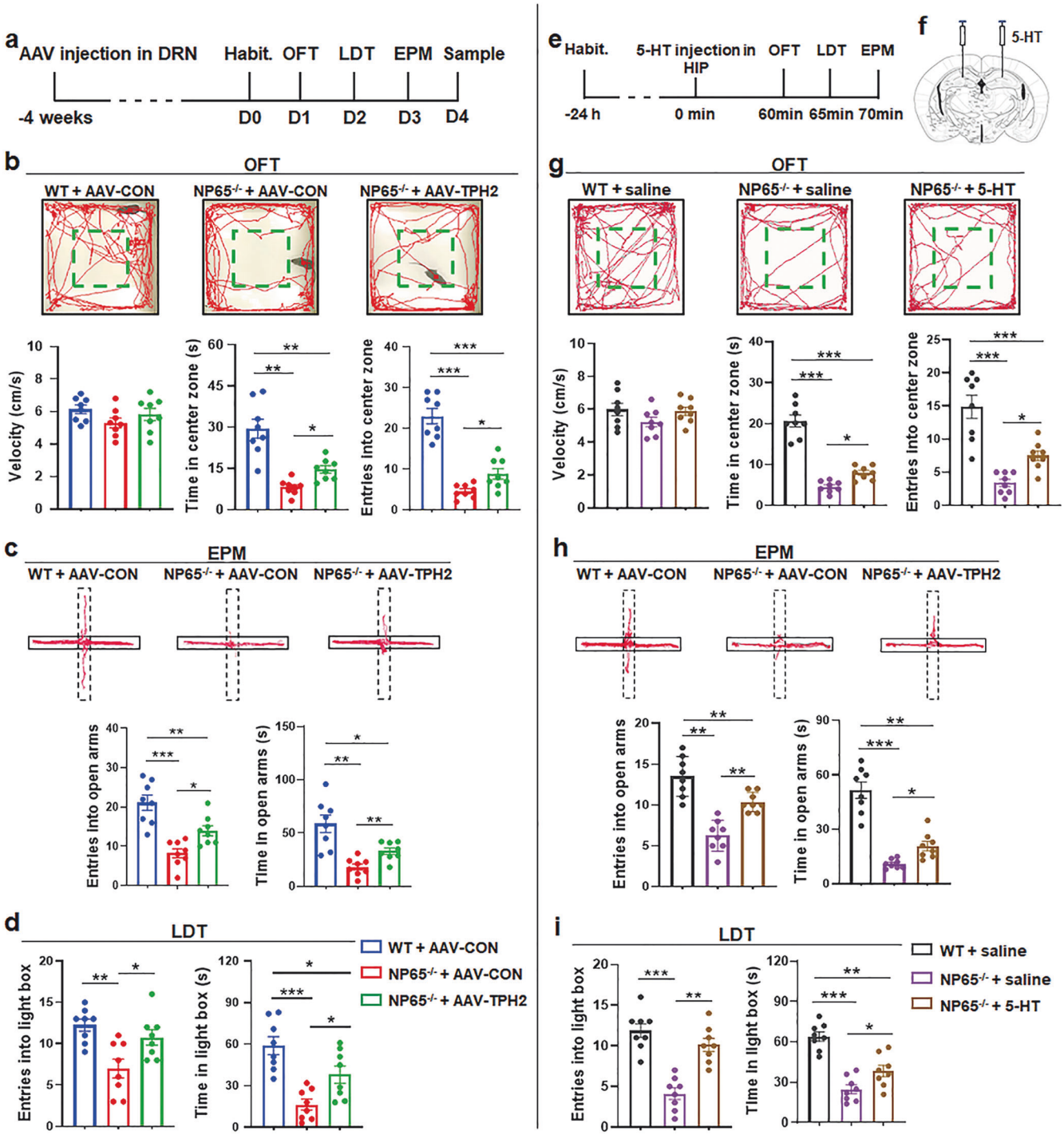

Fig. 2 Administration of AAV-TPH2 in DRN or 5-HT in hippocampus partly alleviates anxiety-like behaviors in NP65$^{-/-}$ mice. a Scheme of assessing anxiety-like behaviors 4 weeks after injection of the AAV-TPH2 or AAV-CON (as control) in DRN of NP65$^{-/-}$ mice ($n = 8$ mice/group). **b** In OFT, the representative tracing patterns (upper panel, the area enclosed by green dotted line is the center zone) and quantification (lower panel) showed the effect of AAV-TPH2 treatment on anxiety-behaviors of NP65$^{-/-}$ mice. **c** In EPM test, the representative tracing patterns (upper panel, dotted line indicates open arms and solid line indicates closed arms) and quantitative analysis (lower panel) displayed the effect of AAV-TPH2 treatment on anxiety-behaviors of NP65$^{-/-}$ mice. **d** LDT test showed the effect of AAV-TPH2 on anxiety-behaviors of NP65$^{-/-}$ mice. **e** Scheme of assessing behaviors 60 min after injection of synthesized 5-HT (20 μg/1 μL or saline (1 μL, as control) in the hippocampus of NP65$^{-/-}$ mice ($n = 8$ mice/group). **f** schematic of 5-HT injection in hippocampus. **g** In the OFT, the representative tracing patterns (upper panel) and quantification (lower panel) exhibited the effect of exogenous 5-HT on the movement speed and entries and time in the center zone of NP65$^{-/-}$ mice. **h** In EPM test, the representative patterns (upper panel, dotted line indicative of open arms) and quantification (lower panel) showed the effect of exogenous 5-HT on entries and time in the open arms of NP65$^{-/-}$ mice. **i** LDT test showed the effect of exogenous 5-HT on entries and time in the light box of NP65$^{-/-}$ mice. Data are presented as mean ± SEM. $^{*}P < 0.05$; $^{**}P < 0.01$; $^{***}P < 0.001$.

NP65$^{-/-}$ mice. Four weeks after viral injection, a serials of anxiety behavioral tests were performed as above and the DRN tissue was collected to measure TPH2 level (Fig. 3a, b). As shown in Fig. 3, NP65$^{-/-}$ mice treated with AAV-CON (NP65$^{-/-}$ control) exhibited anxiety-like behaviors measured by OFT, EPM and LDT tests compared with WT mice treated with AAV-CON (Fig. 3c–e), consistent with our previous reports [2, 3] and the above-mentioned results. As expected, AAV-NP65 treatment in the DRN partly reversed the decrease in the duration in the central zone ($F_{2,18} = 12.652$, $P = 0.039$) and the number of entries into the central zone ($F_{2,18} = 35.419$, $P = 0.029$) in NP65$^{-/-}$ mice in the OFT (Fig. 3c). In the EPM test, AAV-NP65 apparently increased the time spent in the open arms ($F_{2,18} = 16.649$, $P = 0.011$) and the number of entries into the open arms ($F_{2,18} = 31.885$, $P = 0.006$) in NP65$^{-/-}$ mice (Fig. 3d). Lastly, in the LDT test, AAV-NP65 significantly enhanced the time spent in the light box ($F_{2,18} = 31.772$, $P = 0.006$), although the number of entries into light box ($F_{2,18} = 77.452$, $P = 0.181$) was not obviously affected in NP65$^{-/-}$ mice (Fig. 3e). Therefore, these results demonstrate that the administration of AAV-NP65 into the DRN can mitigate anxiety-like behaviors in NP65$^{-/-}$ mice.

Next, DRN tissues were collected to evaluate the expression of NP65 and TPH2. First, NP65 expression was measured using Western blotting. As expected, NP65 expression was detected in WT control but absent in NP65$^{-/-}$ control (Fig. 3f). Notably, NP65 expression was significantly increased in NP65$^{-/-}$ mice treated with AAV-NP65 (Fig. 3f), indicating that AAV-NP65 injection replenishes NP65 expression in DRN of NP65$^{-/-}$ mice. Next, TPH2 expression was also examined in DRN of these mice. Consistent with our previous report [2] and the above results (Fig. 1b, c), NP65$^{-/-}$ control showed a significant decrease in TPH2 expression compared with that in WT control ($F_{2,6} = 44.09$, $P < 0.001$, Fig. 3f, g). Interestingly, administration of AAV-NP65 in DRN significantly enhanced the TPH2 level of DRN in NP65$^{-/-}$ mice ($F_{2,6} = 44.09$, $P = 0.002$, Fig. 3f, g). In addition, immunostaining also revealed a significant decrease in the number of TPH2-positive cells in DRN ($F_{2,6} = 27.04$, $P = 0.008$) and TPH2-positive terminal area in hippocampus ($F_{2,6} = 79.796$, $P = 0.005$) of NP65$^{-/-}$ control compared with those in WT control (Fig. 3h–j), consistent with the results of the Fig. 1d. Notably, the injection of AAV-NP65 in DRN significantly increased the amounts of both TPH2-positive cells in the DRN ($F_{2,6} = 27.04$, $P = 0.043$) and TPH2-positive axonal terminals in the hippocampus ($F_{2,6} = 79.796$, $P = 0.024$) in NP65$^{-/-}$ mice (Fig. 3h–j). Therefore, these results clearly demonstrate that the replenishment of NP65 in the DRN alleviates anxiety-like behaviors in NP65$^{-/-}$ mice, probably through increasing the number of serotoninergic neurons in DRN as well as the 5-HT projection of DRN to the hippocampus.

Administration of HTR3 agonist SR57227A in hippocampus mitigates anxiety-like behaviors in NP65$^{-/-}$ mice

5-HTergic neurons in DRN project to the hippocampus and form synapses with neurons bearing 5-HT receptors to regulate the activity of hippocampal cells [18, 22]. So far, HTR3 has been the only ligand-gated ion channel receptor among all identified 5-HT receptors [31], and is highly expressed in the subtypes of interneurons in the hippocampus and cortex [30, 42–44]. HTR3A is an indispensable subunit of HTR3 and is necessary for functional HTR3 [31]. In our previous study, RNA-sequencing analysis of differentially-expressed genes in hippocampus and qRT-PCR showed a significant decrease in the level of HTR3A mRNA in NP65$^{-/-}$ mice [34]. In addition, Western blots showed a decrease in HTR3A protein levels in forebrain and brainstem of NP65$^{-/-}$ mice [2]. Thus, it is hypothesized that the decreased expression of HTR3A would impair HTR3 function in hippocampus and lower the responses of hippocampus to 5-HT, resulting in the anxiety-like behaviors of mice. To verify this, expression of HTR3A protein of hippocampus and cortex was examined in NP65$^{-/-}$ mice. Western blotting showed a significant reduction in HTR3A level in the hippocampus of NP65$^{-/-}$ mice ($t_4 = 0.001$, Fig. 4a), which was also confirmed by immunostaining analysis exhibiting a statistical decrease in HTR3A-positive area ($t_4 = 0.038$, Fig. 4b, c). These results confirm that HTR3A expression is significantly decreased in the hippocampus of NP65$^{-/-}$ mice. Next, SR57227A, a commonly used HTR3 receptor agonist, was microinjected in bilateral hippocampus of NP65$^{-/-}$ mice, and these mice were subjected to anxiety tests as above 30 min after viral injection (Fig. 4d–g). As controls, administration of SR57227A had no effects on anxiety-like behaviors in WT mice (Fig. 4e–i). Interestingly, in the OFT, SR57227A treatment significantly increased the time spent in the center zone ($F_{3,20} = 36.611$, $P = 0.037$) and the number of entries into the center zone ($F_{3,20} = 24.271$, $P = 0.025$) without affecting the motor ability in NP65$^{-/-}$ mice compared with vehicle control ($F_{3,20} = 0.709$, $P = 0.522$, Fig. 4e, f). In the EPM test, SR57227A administration significantly enhanced the number of entries into the open arms ($F_{3,20} = 20.78$, $P = 0.003$) and the duration in the open arms ($F_{3,20} = 15.342$, $P = 0.01$) in NP65$^{-/-}$ mice (Fig. 4g, h). In the LDT test, administration of SR57227A increased the number of entries into light box ($F_{3,20} = 6.868$, $P = 0.008$) and the time spent in the light box ($F_{3,20} = 56.072$, $P = 0.006$) in NP65$^{-/-}$ mice (Fig. 4i). These data suggest that the impairment of HTR3 receptor probably contributes to the anxiety-like behaviors in NP65$^{-/-}$ mice.

Replenishment of TPH2 in DRN reverses the impaired LTP maintenance in the hippocampus of NP65$^{-/-}$ mice

To further test this view that the reduced 5-HT synaptic transmission from the DRN to the hippocampus may underlie the anxiety-like behaviors of NP65$^{-/-}$ mice, we set to examine the LTP of hippocampal slices four weeks after the administration of AAV-TPH2 in the DRN of NP65$^{-/-}$ mice. Consistent with our previous results and other reports [2, 7], NP65$^{-/-}$ mice treated with the AAV-CON (NP65$^{-/-}$ control) showed a comparable basal synaptic transmission evaluated by fEPSP (Fig. 5a), compared with that in WT control. The amplitudes of fEPSP after train stimulations (100 Hz) in NP65$^{-/-}$ control were initially increased, but rapidly decreased to the baseline level at 60 min after induction compared with WT control ($P < 0.0001$, Fig. 5a). Notably, AAV-TPH2 treatment significantly enhanced fEPSP amplitudes at 60 min after induction in NP65$^{-/-}$ mice (Fig. 5a, $P < 0.001$; Fig. 5b, $P < 0.05$; Fig. 5c, $P < 0.001$). Therefore, these results demonstrate that replenishment of TPH2 in DRN partly repairs the impairment of LTP maintenance in hippocampus of NP65-deficient mice, suggesting that replenishment of TPH2 in DRN enhances 5-HTergic transmission from the DRN to the hippocampus. These results combined with data in Fig. 1 indicate that the increased 5-HTergic transmission from DRN to the hippocampus underlies the alleviated anxiety-like behaviors in NP65$^{-/-}$ mice after TPH2 replenishment in DRN.

NP65 deficiency downregulates TPH2 expression via transcription factor Lmx1b in DRN of adult mice

Our studies have shown a significant reduction in TPH2 protein in the DRN of NP65$^{-/-}$ mice. To differentiate that this reduction is a result of embryonic developmental defects or a consequence of NP65 deficiency in postnatal ages, expression of TPH2 at different stages after birth in NP65$^{-/-}$ mice was explored by immunoblot analysis. At postnatal day 0 (P0), both NP65$^{-/-}$ and WT mice exhibited abundant and similar expression in TPH2 ($t_4 = 0.506$, Fig. 6a, b). However, NP65$^{-/-}$ mice showed a significant reduction in TPH2 levels at P14 ($t_4 = 0.003$, Fig. 6a, b). Additionally, qRT-PCR analysis showed that TPH2 mRNA level was unaffected at P0 ($t_4 = 0.864$) but significantly reduced at P14 ($t_4 = 0.024$) and P28 ($t_4 = 0.033$) in the DRN of NP65$^{-/-}$ mice compared with that in WT mice (Fig. 6c). Thus, these findings indicate that the decrease in

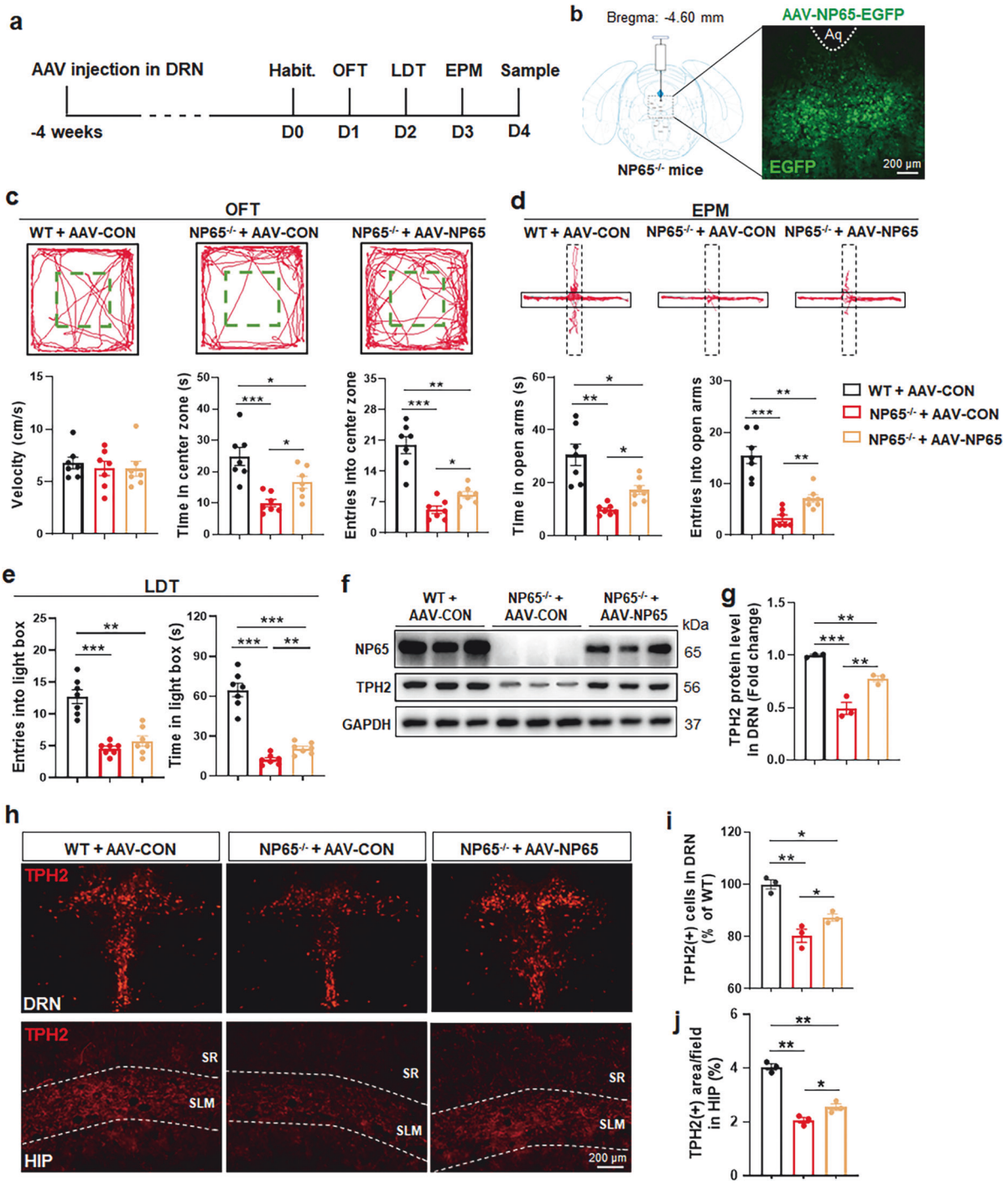

Fig. 3 Administration of AAV-NP65 into the DRN partially alleviates anxiety-like behaviors and increases TPH2 level in DRN and hippocampus in NP65$^{-/-}$ mice. a, **b** Scheme of assessing anxiety-like behaviors 4 weeks after injection of the AAV-NP65 or AAV-CON (as control) in DRN of NP65$^{-/-}$ mice ($n = 7$ mice/group), as indicated (**b**) by EGFP (green) under fluorescence microscopy 4 weeks after virus injection. 100× magnification, Scale bar = 200 μm. **c** In OFT, the representative tracing patterns (upper panel, the area enclosed by green dotted line is the center zone) and quantification (lower panel) showed the effect of AAV-NP65 on the movement speed and entries and time in the center zone of NP65$^{-/-}$ mice. **d** In EPM test, the representative tracing patterns (upper panel, dotted line indicates open arms and solid line indicates closed arms) and quantitative analysis (lower panel) displayed the effect of AAV-NP65 on entries and time in the open arms of NP65$^{-/-}$ mice. **e** In LDT test, the effect of AAV-NP65 on entries and time in the light box of NP65$^{-/-}$ mice. **f** Representative bands of Western blotting for NP65 and TPH2 in DRN ($n = 3$ mice/group). **g** Quantitative analysis of TPH2 bands in DRN of NP65$^{-/-}$ mice after AAV-NP65 treatment. **h**–**j** Representative TPH2 immunostaining images in DRN (upper panel) and stratum lacunosum molecular (SLM) and stratum radiatus (SR) of hippocampus (HIP, lower panel), and quantification of TPH2(+) cells in DRN (**i**) and TPH2(+) axonal terminals in hippocampus (**j**) in NP65$^{-/-}$ mice ($n = 3$ mice/group), 100× magnification, Scale bar = 200 μm. Data are presented as mean ± SEM. *$P < 0.05$; **$P < 0.01$; ***$P < 0.001$.

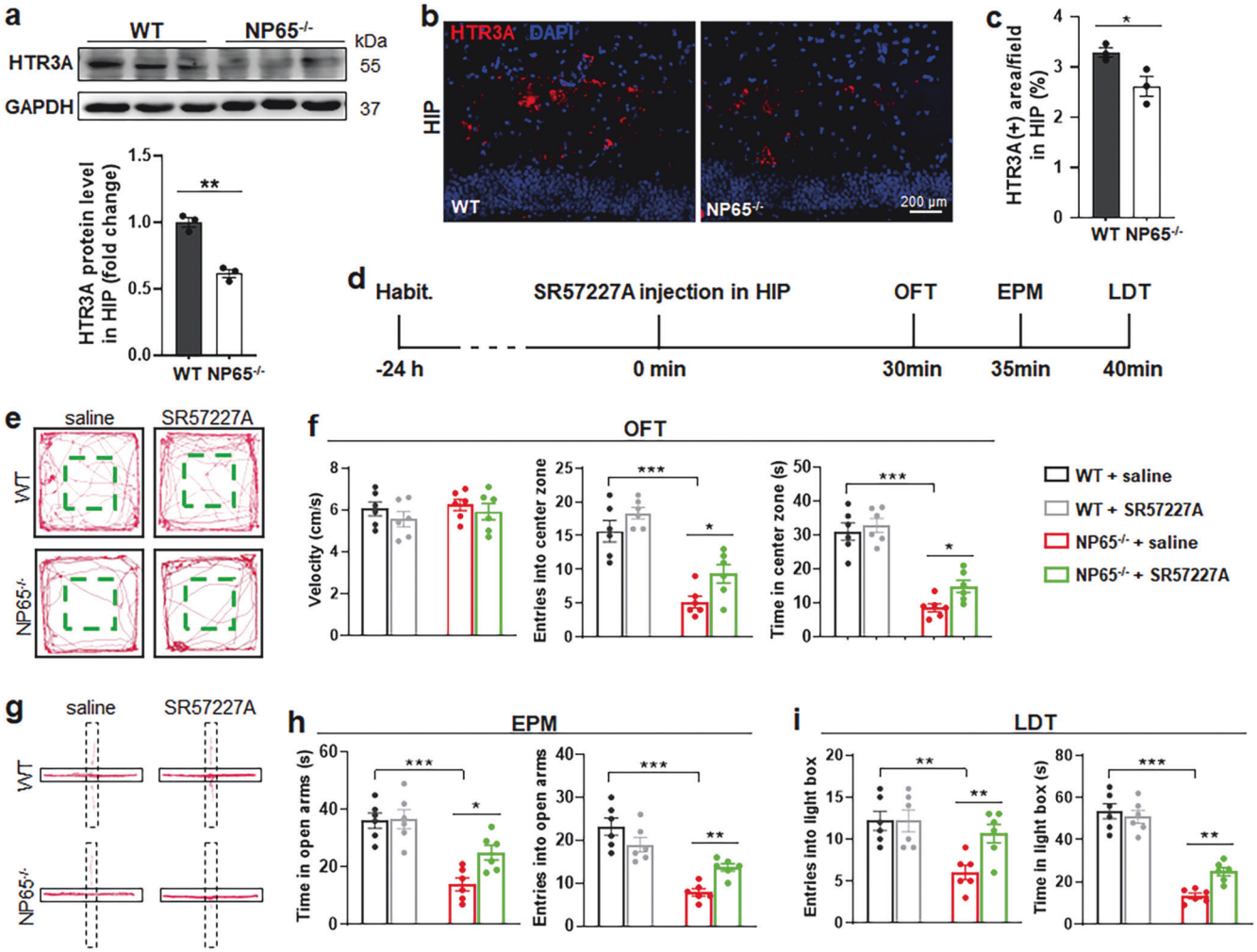

Fig. 4 NP65 deficiency decreases HTR3A level in the hippocampus and HTR3 agonist SR57227A mitigates the anxiety-like behaviors in NP65$^{-/-}$ mice. a Representative immunoreactive bands (upper panel) of HTR3A in the hippocampus (HIP) of WT and NP65$^{-/-}$ mice and quantitative analysis (lower panel) of HTR3A level in NP65$^{-/-}$ mice ($n = 3$ mice/group). Representative immunostaining images (**b**) of HTR3A-positive cells (red) in hippocampus and quantification (**c**) of HTR3A-positive area in NP65$^{-/-}$ mice, nucleus stained with DAPI (blue). 100× magnification, Scale bar = 200 μm. **d** Scheme of assessing anxiety-like behaviors 30 min after injection of HTR3 agonist SR57227A in hippocampus ($n = 6$ mice/group). In OFT, the representative tracing patterns (**e**) and quantification (**f**) showed that effect of SR57227A on the movement speed and entries and time in the center zone of NP65$^{-/-}$ and WT mice. In EPM test, the representative tracing patterns (**g**) and quantitative analysis (**h**) displayed the effect of SR57227A on entries and time in the open arms of NP65$^{-/-}$ and WT mice. **i** In LDT test, the effect of SR57227A on entries and time in the light box of NP65$^{-/-}$ and WT mice. Data are presented as mean ± SEM. *$P < 0.05$, **$P < 0.01$, ***$P < 0.001$.

TPH2 gene expression is attributed to the NP65 deficiency in postnatal mice.

To understand how NP65 modulates TPH2 gene expression, the expression of transcription factors Pet1 and Lmx1b known for regulating the expression of TPH2 [45–48] was examined in NP65$^{-/-}$ mice at adulthood. As shown in Fig. 6d, qRT-PCR analysis showed that the expression of Lmx1b mRNA in DRN was significantly reduced while the level of Pet1 mRNA was unaffected in NP65$^{-/-}$ mice relative to those in WT controls. Furthermore, the expression of Lmx1b was measured in NP65$^{-/-}$ mice at different ages after birth by immunoblots and qRT-PCR analysis. We found that Lmx1b protein ($t_4 = 0.904$, Fig. 6e, f) and mRNA ($t_4 = 0.599$, Fig. 6g) levels were comparable at P0 but significantly decreased at P14 (protein: $t_4 = 0.011$, Fig. 6e, f; mRNA: $t_4 = 0.041$, Fig. 6g) and P28 (protein: $t_4 = 0.001$, Fig. 6e, f; mRNA: $t_4 = 0.036$, Fig. 6g) in NP65$^{-/-}$ mice compared with those in WT mice. Thus, these results suggest that the loss of NP65 downregulates TPH2 expression via affecting the expression of Lmx1b in mice.

To further test this view, double immunostaining for TPH2/NP65 and 5-HT/NP65 was performed in WT mice and our data revealed that a portion of TPH2-positive neurons or 5-HT-positive neurons were also NP65-immunoreactive (Fig. 6h, i). This co-localization of NP65 with both TPH2 and 5-HT provides morphological basis supporting that NP65 deficiency reduces the expression of TPH2 in 5-HTergic neurons of DRN. In addition, the level of Lmx1b protein was determined in NP65$^{-/-}$ mice treated with AAV-NP65 in DRN as mentioned above in Fig. 3. Western blot analysis showed that the level of Lmx1b protein of DRN was significantly reduced in NP65$^{-/-}$ controls compared with that in WT controls ($F_{2,6} = 16.897$, $P = 0.001$, Fig. 6j, k). Interestingly, administration of AAV-NP65 in DRN significantly reversed the decrease in Lmx1b protein level in NP65$^{-/-}$ mice ($F_{2,6} = 16.897$, $P = 0.018$, Fig. 6j, k). Consistently, immunostaining analysis also displayed that AAV-NP65 in DRN significantly reversed the decrease in number of Lmx1b-positive cells in NP65$^{-/-}$ mice ($F_{2,6} = 31.3$, $P = 0.011$, Fig. 6l, m). Combined with the results in Fig. 3e–i, these in vivo data indicate that NP65

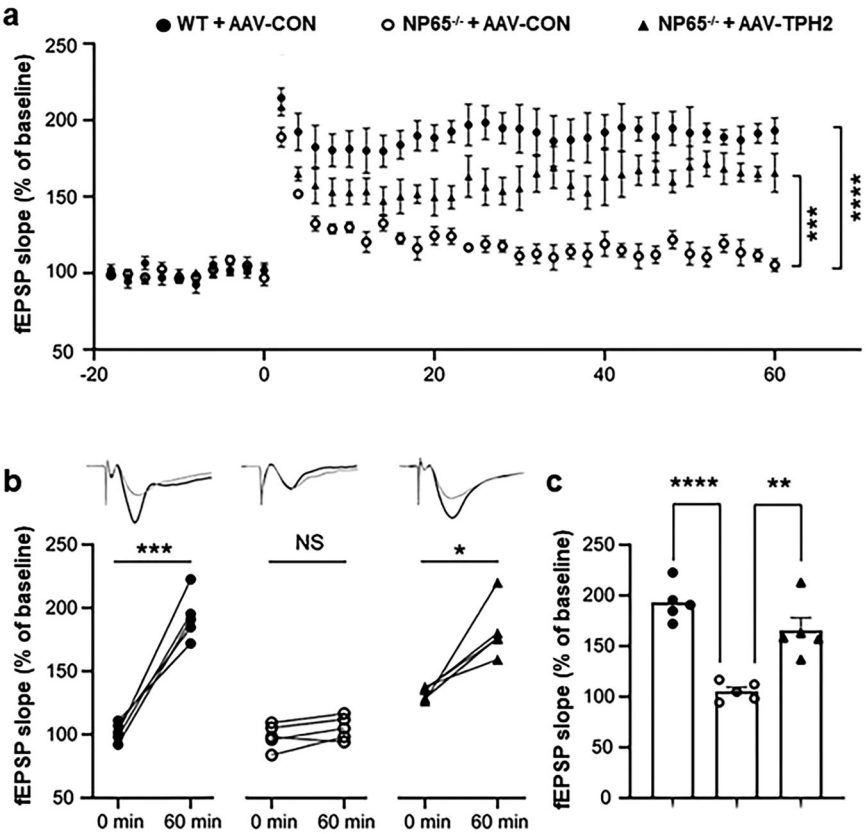

Fig. 5 Injection of AAV-TPH2 in DRN reverses the impaired LTP maintenance in hippocampus of NP65$^{-/-}$ mice. a Average fEPSP elicited in the hippocampus before and after theta-burst stimulation 4 weeks after injection of AAV-TPH2 in DRN of WT and NP65$^{-/-}$ mice. **b** The average of fEPSP slope in WT and NP65$^{-/-}$ mice treated with AAV-TPH2 or AAV-CON and representative time course (upper inserts) of LTP of the fEPSP taken 0 min before and 60 min after tetanus from slices of mice. **c** The average of fEPSP slopes at 60 min after theta-burst stimulation among these groups. Data are shown as mean ± SEM, $n = 5$ mice/group (3-4 slices per mouse). *$P < 0.05$, **$P < 0.01$, ***$P < 0.001$, ****$P < 0.0001$.

deficiency downregulates TPH2 expression via lowering transcription factor Lmx1b in DRN of mice.

DISCUSSION

Our previous studies have shown that NP65$^{-/-}$ mice display a serials of abnormal behaviors, including enhanced spatial memory and social interaction, increased anxiety and reduced depression [2, 3]. Here, we provide evidence for the first time that the decreased serotonergic transmission from DRN to hippocampus leads to the anxiety phenotype of NP65$^{-/-}$ mice.

Relationship of central 5-HT level with anxiety-like behaviors

In spite of extensive investigation, the role of 5-HT is highly controversial in the regulation of anxiety [24, 25, 27, 49–51]. To determine the function of 5-HT in anxiety, a serials of different mutant mice have been generated to completely or dramatically abolish 5-HT in the forebrain, including TPH2$^{-/-}$ mice, Lmx1b$^{-/-}$ mice, Pet1$^{-/-}$ mice, Pet1-Cre;Lmx1b$^{flox/flox}$ mice, Pet1-Cre;TPH2$^{flox/flox}$ mice, and serotonin transporter (Sert)-Cre;vesicular monoamine transporter 2 (Vmat2)$^{flox/flox}$ mice. However, these mutant mice show different behaviors, including normal, anxiolytic-like or anxiogenic-like behaviors [24, 25, 27, 48, 49, 51]. For example, TPH2/TPH1$^{-/-}$ mice had no overt change in marble burying test [28]. 5-HT-deficient mice in the forebrain (TPH2$^{-/-}$ mice, Pet1-Cre;Lmx1b$^{flox/flox}$ mice, Pet1-Cre;TPH2$^{flox/flox}$ mice, and Sert-Cre;Vmat2$^{flox/flox}$ mice) displayed anxiolytic-like behaviors [24, 25, 27, 49, 52], while both the conditional GATA cofactor ZFPM1$^{-/-}$ mice and the conditional Pet1$^{-/-}$ mice had lower concentration of 5-HT in the forebrain and displayed anxiogenic-like behaviors [48, 51]. Given that selective serotonin reuptake inhibitors serve as the clinical front-line treatment for depression and anxiety [53], the results from conditional ZFPM1$^{-/-}$ and Pet1$^{-/-}$ mice suggest that partial loss rather than complete loss of 5-HT in the brain leads to anxiety disorders. In the present study, we provide a serials of evidence showing a causal link between anxiety phenotype and reduced 5-HT levels of hippocampus in NP65$^{-/-}$ mice. First, replenishment of TPH2 in DRN by injection of AAV-TPH2 enhanced 5-HT level in the hippocampus and alleviated anxiety-like behaviors. Second, injection of AAV-NP65 in DRN significantly increased TPH2 expression in DRN and hippocampus, and reduced anxiety-like behaviors. Third, acute administration of exogenous 5-HT in hippocampus decreased anxiety-like behaviors. All these results reveal that the decrease in 5-HT level of hippocampus contributes to the anxiety-like phenotype of NP65$^{-/-}$ mice.

Reduced 5-HT/HTR3 transmission from DRN to hippocampus

Accumulating evidence shows that the DRN is heterogeneous in cell morphology, projecting targets and distinct aspects of behavioral regulation in mice [15, 16, 21, 51, 54–59]. For example, gain- and loss-of-function experiments suggest that amygdala-projecting DRN serotonergic neurons promote anxiety-like behaviors and conditioned fear behaviors [57], while frontal cortex-projecting DRN serotonergic neurons promote active coping in the face of challenge without affecting anxiety-like behaviors in mice [21]. Another report showed that ventral tegmental nucleus- or the bed nucleus of the stria terminalis-projecting DRN serotonergic neurons in mice responded more to stimuli in sucrose reward, the EPM test, foot shock and the first social interaction with a novel mouse, respectively [58]. Notably, we found that replenishment of NP65 or TPH2 in DRN reversed the decrease in TPH2 expression in DRN as well as hippocampus of

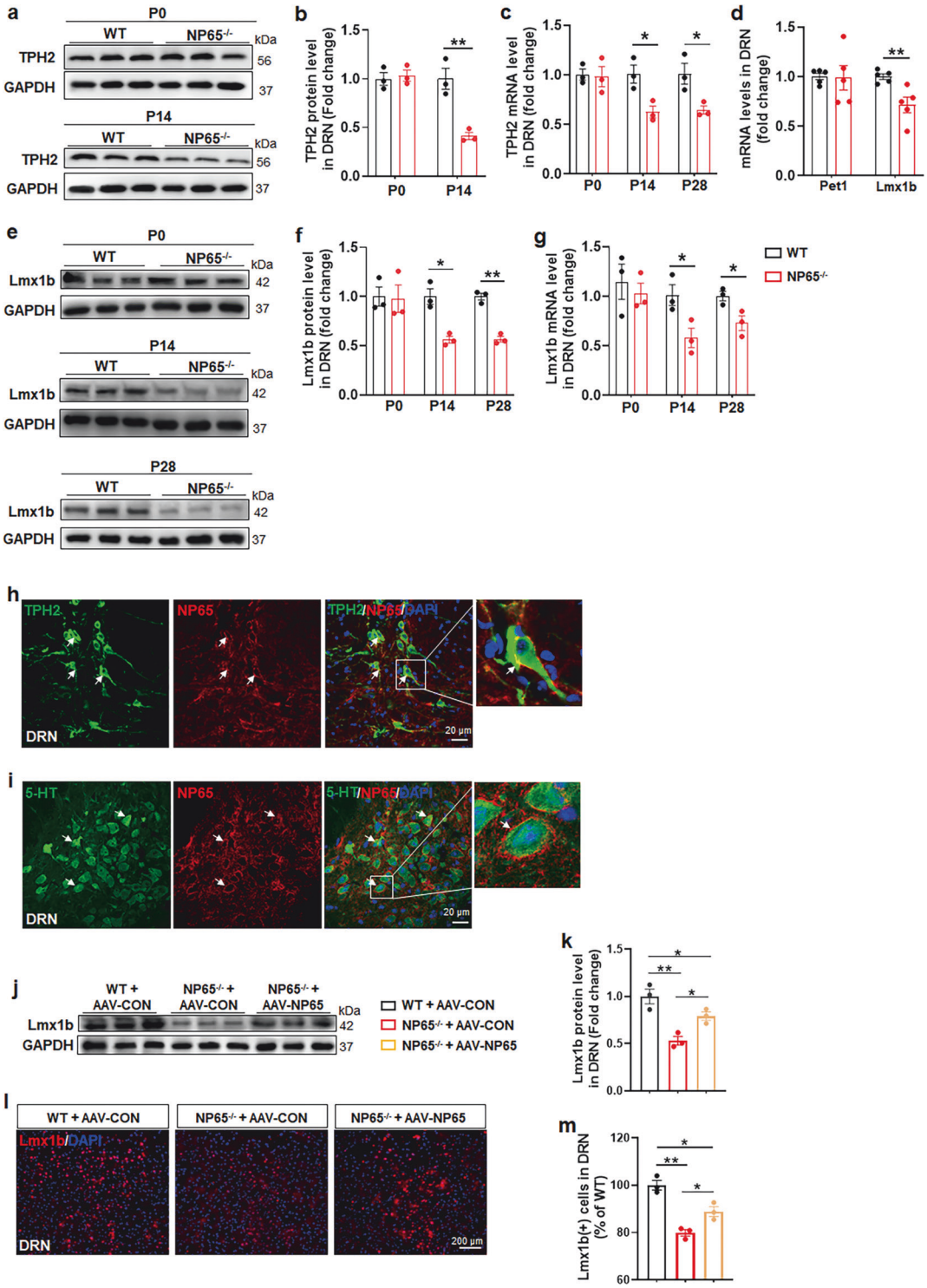

Fig. 6 NP65 deficiency downregulates TPH2 expression via transcription factor Lmx1b in mice. Representative immunoreactive bands of TPH2 bands (**a**) from DRN of WT and NP65$^{-/-}$ mice at postnatal day 0 (P0) and postnatal day 14 (P14), and quantitative analysis (**b**). **c** qRT-PCR analysis showed the expressions of TPH2 mRNA at P0, P14 and P28 in the DRN of NP65$^{-/-}$ mice ($n = 3$ mice/group). **d** qRT-PCR analysis showed the expressions of Lmx1b and Pet1 mRNA in the DRN of NP65$^{-/-}$ mice at adults ($n = 5$ mice/group). Representative immunoreactive bands (**e**) of Lmx1b from DRN of WT and NP65$^{-/-}$ mice at P0, P14 and P28, quantitative analysis (**f**) ($n = 3$ mice/group). **g** qRT-PCR analysis showed that the expressions of Lmx1b mRNA at P0, P14 and P28 in the DRN of NP65$^{-/-}$ and WT mice ($n = 3$ mice/group). Typical immunostaining of TPH2/NP65 (**h**) and 5-HT/NP65 (**i**) in DRN of WT mice, arrow indicating double-staining. Right panel: magnification of the white square area from the left panel. 600× magnification, Scale bar = 20 μm. Representative Lmx1b immunoblots (**j**) of Western blotting and quantification (**k**) of Lmx1b level in DRN. Representative Lmx1b immunostaining (**l**) and quantification (**m**) of the amounts of Lmx1b-positive cells in DRN of NP65$^{-/-}$ mice, nucleus stained with DAPI. 100× magnification, Scale bar = 200 μm. Data are shown as mean ± SEM. *$P < 0.05$, **$P < 0.01$.

NP65$^{-/-}$ mice and mitigated anxiety-like behaviors. In addition, the replenishment of TPH2 in DRN significantly increased the concentrations of 5-HT in DRN and hippocampus but not in frontal cortex and partly repaired the impairment of LTP in hippocampus of NP65$^{-/-}$ mice. Thus, these results reveal that reduced 5-HT signaling from the DRN to hippocampus leads to the anxiogenic phenotype of NP65$^{-/-}$ mice. Furthermore, distinct postsynaptic subtypes of HTR determine the function and behaviors in 5-HT signaling transmission throughout brain [29, 30, 60]. Our previous studies reported the reduced expression of HTR3A in hippocampus of NP65$^{-/-}$ mice [2, 34], and this present study confirmed that acute application of HTR3 agonist SR57227A significantly normalized the anxiety phenotype in NP65-deficient mice. Taken together, our study demonstrates for the first time that NP65 deficiency leads to the reduced serotonergic-HTR3 transmission from the DRN to hippocampus, which partially contributes to the anxiety phenotype in mice.

The underlying mechanism for how NP65 regulates TPH2 expression

Next, we further verified that the reduced expression in TPH2 of NP65 $^{-/-}$ mice was due to the loss of NP65 in postanal stage rather than its deletion during embryonic development based on the data that TPH2 level in NP65$^{-/-}$ mice was comparable at P0, but significantly lowered at P14 and P28 compared with WT mice. NP65/TPH2 co-colocalization in DRN of WT mice also suggests a possibility that NP65 could mediate TPH2 expression in serotonergic neurons. Transcription factors Lmx1b and Pet1 are essential for differentiation of serotonergic neurons [45, 47, 48, 61, 62] and persistently expressed in serotonergic neurons at adulthood to regulate serotonergic function [45, 61]. Given the significance of Lmx1b and Pet1, we thus examined the level of Lmx1b and Pet1 in NP65$^{-/-}$ mice and found a significant decrease in Lmx1b mRNA level but similar level in Pet1 mRNA in NP65$^{-/-}$ mice. Our data indicate that downregulation of Lmx1b mRNA due to loss of NP65 results in the decrease of TPH2 expression. Because Pet1 acts downstream of Lmx1b in controlling maturation of serotonergic neurons [47], our results are reasonable and consistent with above mentioned reports in which Lmx1b$^{-/-}$ or Pet1-Cre;Lmx1b$^{flox/flox}$ mutant mice displayed complete loss of TPH2 and 5-HT levels [47, 63]. Our results were also supported by another report in which conditional knockout of Lmx1b induced by tamoxifen in Pet1-CreER^{T2};Lmx1b$^{flox/flox}$ mice led to reduction of 5-HT level, and the decreased expression of TPH2, Sert and Vmat2 [26]. To further verify our results, Lmx1b protein level was assessed in NP65$^{-/-}$ mice with administration of AAV-NP65 in DRN. More importantly, AAV-NP65 in DRN significantly increased the level of Lmx1b protein in NP65$^{-/-}$ mice. Lastly, we found that Lmx1b expression was comparable at P0, but significantly decreased at P14 and P28 in NP65$^{-/-}$ mice compared with WT mice measured by Western blots and qRT-PCR. Thus, these results indicate that loss of NP65 in postnatal rather than in embryonic stages results in a decrease in Lmx1b expression, which determines the temporal expression of TPH2.

In conclusion, we have revealed that NP65 deficiency leads to the reduced serotonergic-HTR3 transmission from DRN to hippocampus, which results in anxiety phenotype in mice. In addition, NP65 deficiency downregulates TPH2 expression via affecting the expression of Lmx1b in DRN of adult mice. Future studies are needed to identify the exact mechanism for how NP65 regulates the expression of Lmx1b in mice. These findings provide a novel and insightful view about the NP65 function and the molecular mechanism about anxiogenic-like behaviors in mice.

ACKNOWLEDGEMENTS

This work was supported by National Natural Science Foundation of China (81371213 and 81070987) and by grants from the Natural Science Foundation of Shanghai (21ZR1468400).

AUTHOR CONTRIBUTIONS

QLY designed the experiments and wrote the manuscript. JC, LC, YNZ, JL and XMZ performed the experiments. LZ and LH analyzed the data. All authors contributed to the article and approved the submitted version.

ADDITIONAL INFORMATION

Competing interests: The authors declare no competing interests.

REFERENCES

1. Bandelow B, Michaelis S. Epidemiology of anxiety disorders in the 21st century. Dialogues Clin Neurosci. 2015;17:327–35.
2. Li HH, Liu YT, Gao XQ, Liu LF, Amuti S, Wu DD, et al. Neuroplastin 65 modulates anxiety- and depression-like behavior likely through adult hippocampal neurogenesis and central 5-HT activity. FEBS J. 2019;286:3401–15.
3. Amuti S, Tang YC, Wu S, Liu LF, Huang L, Zhang HB, et al. Neuroplastin 65 mediates cognitive functions via excitatory/inhibitory synapse imbalance and ERK signal pathway. Neurobiol Learn Mem. 2016;127:72–83.
4. Hill IE, Selkirk CP, Hawkes RB, Beesley PW. Characterization of novel glycoprotein components of synaptic membranes and postsynaptic densities, gp65 and gp55, with a monoclonal antibody. Brain Res. 1988;461:27–43.
5. Langnaese K, Beesley PW, Gundelfinger ED. Synaptic membrane glycoproteins gp65 and gp55 are new members of the immunoglobulin superfamily. J Biol Chem. 1997;272:821–7.
6. Langnaese K, Mummery R, Gundelfinger ED, Beesley PW. Immunoglobulin superfamily members gp65 and gp55: tissue distribution of glycoforms. FEBS Lett. 1998;429:284–8.
7. Smalla KH, Matthies H, Langnäse K, Shabir S, Böckers TM, Wyneken U, et al. The synaptic glycoprotein neuroplastin is involved in long-term potentiation at hippocampal CA1 synapses. Proc Natl Acad Sci USA. 2000;97:4327–32.
8. Bernstein HG, Smalla KH, Bogerts B, Gordon-Weeks PR, Beesley PW, Gundelfinger ED, et al. The immunolocalization of the synaptic glycoprotein neuroplastin differs substantially between the human and the rodent brain. Brain Res. 2007;1134:107–12.
9. Bhattacharya S, Herrera-Molina R, Sabanov V, Ahmed T, Iscru E, Stöber F, et al. Genetically induced retrograde amnesia of associative memories after neuroplastin ablation. Biol Psychiatry. 2017;81:124–35.
10. Lowry CA, Johnson PL, Hay-Schmidt A, Mikkelsen J, Shekhar A. Modulation of anxiety circuits by serotonergic systems. Stress. 2005;8:233–46.
11. Hale MW, Shekhar A, Lowry CA. Stress-related serotonergic systems: implications for symptomatology of anxiety and affective disorders. Cell Mol Neurobiol. 2012;32:695–708.
12. Teissier A, Chemiakine A, Inbar B, Bagchi S, Ray RS, Palmiter RD, et al. Activity of raphé serotonergic neurons controls emotional behaviors. Cell Rep. 2015;13:1965–76.
13. Dolzani SD, Baratta MV, Amat J, Agster KL, Saddoris MP, Watkins LR, et al. Activation of a Habenulo-Raphe circuit is critical for the behavioral and neurochemical consequences of uncontrollable stress in the male rat. eNeuro. 2016;3:e0229.
14. Nishitani N, Nagayasu K, Asaoka N, Yamashiro M, Andoh C, Nagai Y, et al. Manipulation of dorsal raphe serotonergic neurons modulates active coping to inescapable stress and anxiety-related behaviors in mice and rats. Neuropsychopharmacology. 2019;44:721–32.
15. Liu J, Zhou Y, Li Y, Hu F, Lu Y, Ma M, et al. Dorsal raphe neurons signal reward through 5-HT and glutamate. Neuron. 2014;81:1360–74.
16. Luo M, Zhou J, Liu Z. Reward processing by the dorsal raphe nucleus: 5-HT and beyond. Learn Mem. 2015;22:452–60.
17. Ishimura K, Takeuchi Y, Fujiwara K, Tominaga M, Yoshioka H, Sawada T. Quantitative analysis of the distribution of serotonin-immunoreactive cell bodies in the mouse brain. Neurosci Lett. 1988;91:265–70.
18. Abrams JK, Johnson PL, Hollis JH, Lowry CA. Anatomic and functional topography of the dorsal raphe nucleus. Ann N Y Acad Sci. 2004;1018:46–57.
19. Pourhamzeh M, Moravej FG, Arabi M, Shahriari E, Mehrabi S, Ward R, et al. The roles of serotonin in neuropsychiatric disorders. Cell Mol Neurobiol. 2022;42:1671–92.
20. Liu LF, Liu YT, Wu DD, Cheng J, Li NN, Zheng YN, et al. Inhibiting 5-hydroxytryptamine receptor 3 alleviates pathological changes of a mouse model of Alzheimer's disease. Neural Regen Res. 2023;18:2019–28.
21. Ren J, Friedmann D, Xiong J, Liu CD, Ferguson BR, Weerakkody T, et al. Anatomically defined and functionally distinct dorsal raphe serotonin sub-systems. Cell. 2018;175:472–87.
22. Bang SJ, Jensen P, Dymecki SM, Commons KG. Projections and interconnections of genetically defined serotonin neurons in mice. Eur J Neurosci. 2012;35:85–96.
23. Zhang X, Beaulieu JM, Sotnikova TD, Gainetdinov RR, Caron MG. Tryptophan hydroxylase-2 controls brain serotonin synthesis. Science. 2004;305:217.

24. Song NN, Jia YF, Zhang L, Zhang Q, Huang Y, Liu XZ, et al. Reducing central serotonin in adulthood promotes hippocampal neurogenesis. Sci Rep. 2016;6:20338.
25. Jia YF, Song NN, Mao RR, Li JN, Zhang Q, Huang Y, et al. Abnormal anxiety- and depression-like behaviors in mice lacking both central serotonergic neurons and pancreatic islet cells. Front Behav Neurosci. 2014;8:325.
26. Song NN, Xiu JB, Huang Y, Chen JY, Zhang L, Gutknecht L, et al. Adult raphe-specific deletion of Lmx1b leads to central serotonin deficiency. PLoS One. 2011;6:e15998.
27. Dai JX, Han HL, Tian M, Cao J, Xiu JB, Song NN, et al. Enhanced contextual fear memory in central serotonin-deficient mice. Proc Natl Acad Sci USA. 2008;105:11981–6.
28. Savelieva KV, Zhao S, Pogorelov VM, Rajan I, Yang Q, Cullinan E, et al. Genetic disruption of both tryptophan hydroxylase genes dramatically reduces serotonin and affects behavior in models sensitive to antidepressants. PLoS One. 2008;3:e3301.
29. Naughton M, Mulrooney JB, Leonard BE. A review of the role of serotonin receptors in psychiatric disorders. Hum Psychopharmacol. 2000;15:397–415.
30. Barnes NM, Sharp T. A review of central 5-HT receptors and their function. Neuropharmacology. 1999;38:1083–152.
31. Maricq AV, Peterson AS, Brake AJ, Myers RM, Julius D. Primary structure and functional expression of the 5HT3 receptor, a serotonin-gated ion channel. Science. 1991;254:432–7.
32. Heisler LK, Chu HM, Brennan TJ, Danao JA, Bajwa P, Parsons LH, et al. Elevated anxiety and antidepressant-like responses in serotonin 5-HT_{1A} receptor mutant mice. Proc Natl Acad Sci USA. 1998;95:15049–54.
33. Kelley SP, Bratt AM, Hodge CW. Targeted gene deletion of the 5-HT_{3A} receptor subunit produces an anxiolytic phenotype in mice. Eur J Pharmacol. 2003;461:19–25.
34. Li HH, Zeng JJ, Huang L, Wu DD, Liu LF, Liu YT, et al. Microarray analysis of gene expression changes in neuroplastin 65-knockout mice: implications for abnormal cognition and emotional disorders. Neurosci Bull. 2018;34:779–88.
35. Mota CM, Borges GS, Amorim MR, Carolino ROG, Batalhão ME, Anselmo-Franci JA, et al. Central serotonin prevents hypotension and hypothermia and reduces plasma and spleen cytokine levels during systemic inflammation. Brain Behav Immun. 2019;80:255–65.
36. Voronova IP, Naumenko VS, Khramova GM, Kozyreva TV, Popova NK. Central 5-HT_3 receptor-induced hypothermia is associated with reduced metabolic rate and increased heat loss. Neurosci Lett. 2011;504:209–14.
37. Fletcher PJ, Davies M. Dorsal raphe microinjection of 5-HT and indirect 5-HT agonists induces feeding in rats. Eur J Pharmacol. 1990;184:265–71.
38. Li XH, Matsuura T, Xue M, Chen QY, Liu RH, Lu JS, et al. Oxytocin in the anterior cingulate cortex attenuates neuropathic pain and emotional anxiety by inhibiting presynaptic long-term potentiation. Cell Rep. 2021;36:109411.
39. Prut L, Belzung C. The open field as a paradigm to measure the effects of drugs on anxiety-like behaviors: a review. Eur J Pharmacol. 2003;463:3–33.
40. Walf AA, Frye CA. The use of the elevated plus maze as an assay of anxiety-related behavior in rodents. Nat Protoc. 2007;2:322–8.
41. Crawley JN. Neuropharmacologic specificity of a simple animal model for the behavioral actions of benzodiazepines. Pharmacol Biochem Behav. 1981;15:695–9.
42. Morales M, Bloom FE. The 5-HT3 receptor is present in different subpopulations of GABAergic neurons in the rat telencephalon. J Neurosci. 1997;17:3157–67.
43. Koyama Y, Kondo M, Shimada S. Building a 5-HT_{3A} receptor expression map in the mouse brain. Sci Rep. 2017;7:42884.
44. Tecott LH, Maricq AV, Julius D. Nervous system distribution of the serotonin 5-HT_3 receptor mRNA. Proc Natl Acad Sci USA. 1993;90:1430–4.
45. Liu, Maejima T, Wyler SC, Casadesus G, Herlitze S, Deneris ES. Pet-1 is required across different stages of life to regulate serotonergic function. Nat Neurosci. 2010;13:1190–8.
46. Deneris ES, Wyler SC. Serotonergic transcriptional networks and potential importance to mental health. Nat Neurosci. 2012;15:519–27.
47. Ding YQ, Marklund U, Yuan W, Yin J, Wegman L, Ericson J, et al. Lmx1b is essential for the development of serotonergic neurons. Nat Neurosci. 2003;6:933–8.
48. Hendricks TJ, Fyodorov DV, Wegman LJ, Lelutiu NB, Pehek EA, Yamamoto B, et al. Pet-1 ETS gene plays a critical role in 5-HT neuron development and is required for normal anxiety-like and aggressive behavior. Neuron. 2003;37:233–47.
49. Mosienko V, Bert B, Beis D, Matthes S, Fink H, Bader M, et al. Exaggerated aggression and decreased anxiety in mice deficient in brain serotonin. Transl Psychiatry. 2012;2:e122.
50. Abela AR, Browne CJ, Sargin D, Prevot TD, Ji XD, Li Z, et al. Median raphe serotonin neurons promote anxiety-like behavior via inputs to the dorsal hippocampus. Neuropharmacology. 2020;168:107985.
51. Tikker L, Casarotto P, Singh P, Biojone C, Piepponen TP, Estartús N, et al. Inactivation of the GATA cofactor ZFPM1 results in abnormal development of dorsal raphe serotonergic neuron subtypes and increased anxiety-like behavior. J Neurosci. 2020;40:8669–82.
52. Narboux-Nême N, Sagné C, Doly S, Diaz SL, Martin CB, Angenard G, et al. Severe serotonin depletion after conditional deletion of the vesicular monoamine transporter 2 gene in serotonin neurons: neural and behavioral consequences. Neuropsychopharmacology. 2011;36:2538–50.
53. Bandelow B, Michaelis S, Wedekind D. Treatment of anxiety disorders. Dialogues Clin Neurosci. 2017;19:93–107.
54. Calizo LH, Akanwa A, Ma X, Pan YZ, Lemos JC, Craige C, et al. Raphe serotonin neurons are not homogenous: electrophysiological, morphological and neurochemical evidence. Neuropharmacology. 2011;61:524–43.
55. Huang KW, Ochandarena NE, Philson AC, Hyun M, Birnbaum JE, Cicconet M, et al. Molecular and anatomical organization of the dorsal raphe nucleus. Elife. 2019;8:e46464.
56. Ohmura Y, Tsutsui-Kimura I, Sasamori H, Nebuka M, Nishitani N, Tanaka KF, et al. Different roles of distinct serotonergic pathways in anxiety-like behavior, antidepressant-like, and anti-impulsive effects. Neuropharmacology. 2020;167:107703.
57. Bernabe CS, Caliman IF, Truitt WA, Molosh AI, Lowry CA, Hay-Schmidt A, et al. Using loss- and gain-of-function approaches to target amygdala-projecting serotonergic neurons in the dorsal raphe nucleus that enhance anxiety-related and conditioned fear behaviors. J Psychopharmacol. 2020;34:400–11.
58. Paquelet GE, Carrion K, Lacefield CO, Zhou P, Hen R, Miller BR. Single-cell activity and network properties of dorsal raphe nucleus serotonin neurons during emotionally salient behaviors. Neuron. 2022;110:2664–79.
59. Yu XD, Zhu Y, Sun QX, Deng F, Wan J, Zheng D, et al. Distinct serotonergic pathways to the amygdala underlie separate behavioral features of anxiety. Nat Neurosci. 2022;25:1651–63.
60. Lesch KP, Waider J. Serotonin in the modulation of neural plasticity and networks: implications for neurodevelopmental disorders. Neuron. 2012;76:175–91.
61. Dai JX, Hu ZL, Shi M, Guo C, Ding YQ. Postnatal ontogeny of the transcription factor Lmx1b in the mouse central nervous system. J Comp Neurol. 2008;509:341–55.
62. Cheng L, Chen CL, Luo P, Tan M, Qiu M, Johnson R, et al. Lmx1b, Pet-1, and Nkx2.2 coordinately specify serotonergic neurotransmitter phenotype. J Neurosci. 2003;23:9961–7.
63. Zhao ZQ, Scott M, Chiechio S, Wang JS, Renner KJ, Gereau RWT, et al. Lmx1b is required for maintenance of central serotonergic neurons and mice lacking central serotonergic system exhibit normal locomotor activity. J Neurosci. 2006;26:12781–8.